Turbulence Evolution and Transport Behavior During Current Ramp-Up in ITER-Like Plasmas on DIII-D

G.R. McKee[1], M. Austin[2], J. Boedo[3], R. Bravenec[4], C. Holland[3], G. Jackson[5], T.C. Luce[5], T.L. Rhodes[6], D. Rudakov[3], G. Wang[6], Z. Yan[1], L. Zeng[6], and Y. Zhao[1,7]

[1]University of Wisconsin-Madison, 1500 Engineering Dr., Madison, WI 53706-1687, USA
[2]University of Texas-Austin, Austin, Texas, USA
[3]University of California San Diego, 9500 Gilman Dr., La Jolla, CA 92093-0417, USA
[4]Fourth State Research, 503 Lockhart Dr., Austin, TX 78704, USA
[5]General Atomics, PO Box 85608, San Diego, CA 92186-5608, USA
[6]University of California Los Angeles, PO Box 957099, Los Angeles, CA 90095-7099, USA
[7]Suzhou University, Suzhou, China

E-mail contact of main author: george.mckee@wisc.edu

Abstract. Low-wavenumber density fluctuations exhibit unique characteristics during the current ramp-up phase of ITER-like discharges that can partially explain the challenges of correctly modeling transport behavior and predicting global plasma parameters during this period. A strong interaction takes place between the evolving transport, safety factor (q) and kinetic profiles as well as the appearance and evolution of low-order rational surfaces. Density fluctuations from $0.75<\rho<0.9$ are transiently reduced to exceptionally low levels during early times and from $0.8<\rho<0.9$ at late times in the ramp-up in a manner that is different from behavior observed during steady-state plasma conditions with similar values of q_{95}. Turbulence is suppressed as low-order-rational q-surfaces enter the plasma; the local electron temperature likewise exhibits transient increases during these periods of reduced fluctuations indicating changes in transport that impact temperature and consequently the evolution of current density and plasma inductance. These observations can explain discrepancies between CORSICA modelling and the higher electron temperature found previously over the outer half radius. Comparison of turbulence properties with time-varying linear growth rates with GYRO and GENE demonstrate qualitative consistency with measured fluctuation levels, but calculations don't exhibit reduced growth rates near low-order rational surfaces, which is inconsistent with experimental observations. This indicates a mechanism that can contribute to reconciling observed turbulence behavior with transport models, allowing for the development of more accurate predictive tools.

1. Introduction

Understanding transport during the current ramp-up phase of tokamak burning plasmas will be especially crucial to controlling discharge development and predicting plasma duration owing to the large inductive flux consumed during ramp up, and current and voltage limits of the Ohmic and poloidal field coils. Of some concern, transport models of the current ramp-up phase of ITER-similar discharges have shown modest to significant discrepancies with measurements, particularly for the evolution of the electron temperature profile in the outer half radius, where most flux is consumed. This study presents measurements of long-wavelength turbulence, kinetic profiles and transport analysis during the current ramp-up phase for ITER-similar discharges and examines linear gyrokinetic characteristics. These results will be used in future work to test various models with a goal to improve confidence in and accuracy of simulations of the internal inductance, li(3), q-profile and temperature profile evolution during the ramp-up. Here, li(3) is defined as in recent publications pertaining to ITER [1].

Standard ITER discharges will be ramped up to a plasma current of 15 MA during an approximately 110 second phase at a central toroidal field of $B_{T,0}$=5.3 T. The evolution of electron and ion temperature profiles, density, current density, internal inductance and q-

profile during ramp-up will be determined by applied loop voltage, and transport of heat, particles, and current during this rapidly evolving phase. These parameters exhibit strong nonlinear dependencies. Recent experiments on DIII-D [2, 3] and other tokamaks [4, 5] have sought to simulate an ITER-like ramp-up in order to test these models, as well as to optimize the ramp-up scenario [6].

The internal inductance of the plasma during the ramp-up phase directly impacts the currents required in the ohmic and poloidal field coils supplies, and likewise affects the vertical stability. Modeling of transport during the ramp-up phases of DIII-D discharges with CORSICA has shown generally reasonable overall agreement between electron temperature profile evolution, however calculations of internal inductance based on the modeled temperature profile evolution show notable discrepancies [7]. If the measured electron temperature profile is prescribed into CORSICA, then the resulting internal inductance calculation agrees relatively well with that obtained from EFIT and associated profile analysis. This suggests that the neoclassical current diffusivity calculation is sufficiently accurate. The predicted electron temperature, however, is typically calculated to be modestly lower in the outer radius than is measured, which in turn affects the ohmically-driven current density profile and inductance. These anomalies are investigated from the standpoint of turbulence evolution and behavior. Here, the Coppi-Tang transport model was employed in CORSICA and found to have especially large discrepancies near the outer radial regions of the plasma, $\rho>0.6$. This is the zone that has the most impact on current diffusion and internal inductance and so modest errors in the modeled and measured electron temperature in this outer radial zone have significant impact on the calculated inductance.

Different transport models have been implemented and tested in CORSICA and all have been found to be deficient to varying degrees. The Coppi-Tang model was used [7] due to its relative simplicity, full-radius application and rapid convergence. Other models, including a Bohm-gyroBohm model, GLF23, TGLF, Current-Diffusive Ballooning Mode, and Multi-Mode transport model, were tested as part of an ITPA Transport and Confinement Joint Activity [8] with mixed success.

A ‘shortfall’ in predicted transport [9] is found in GYRO simulations: a systematic under-prediction of turbulence and heat transport is found, particularly in the outer radial regions and at higher q_{95} [10]. This under-prediction is in the opposite direction of the CORSICA ramp-up transport modeling here, since electron thermal transport is over-estimated during the ramp, however it is consistent with deficiencies seen with other transport models. The magnitude of this transport shortfall observed in gyrokinetic codes is not, however, universal: GENE simulations of the same DIII-D L-mode discharge parameters [11] demonstrated a smaller transport ‘shortfall’ and could achieve quantitative agreement with modest increases in gradients near $\rho=0.7$. These code-to-code discrepancies are being further investigated. Furthermore, similar studies on the C-MOD tokamak demonstrated reasonably good quantitative agreement of ion transport parameters between experiment and simulation, while electron transport showed mixed agreement and fluctuation measurements were not available [12]. The experimental parameters and transport analysis are presented in Section 2; Section 3 presents fluctuation data during the current–ramp phase; linear gyrokinetic growth rates and frequency spectra are shown in Section 4, and results summarized and conclusions discussed in Section 5.

2. Current Ramp-Up Experiment

ITER similar shape plasmas were developed on DIII-D [2, 3] to characterize performance and

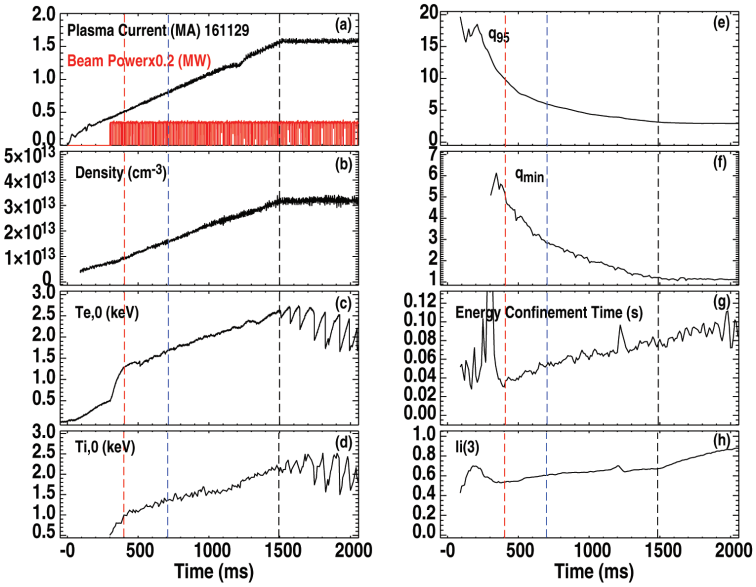

FIG. 1. Time evolution of current ramp experiment showing (a) Ip and neutral beam injection, (b) line-averaged density, (c) central electron temperature, (d) central ion temperature, (e) q_{95}, (f) q_{min}, (g) energy confinement time, and (h) inductance, li(3).

measure turbulence and transport characteristics. Comparison of these fluctuations, transport and kinetic profiles with models and nonlinear simulation seeks to develop an improved transport model that incorporates the unique characteristics of the ramp-up phase. The experiment was performed at appropriately scaled and normalized parameters relative to ITER: B_T=-2.0 T, $I_{P,MAX}$=1.6 MA, $q_{95,min}$=3.1, major radius R_{MAJ}=1.74 m and minor radius, a=0.57 m. The resulting L/R time ratios are near 50, so the anticipated 110 sec ITER current rise time scales to about 2.0 sec. A rise-time of 1.5 sec was used in these experiments to examine the impact of a faster ramp-up, which may reduce initial ohmic flux consumption.

The basic discharge parameters are presented in Fig. 1 showing the current ramp-up phase (t=0-1.5 sec) and major parameters including: line-averaged density, central electron and ion temperatures, q_{95}, q_{min}, energy confinement time, and inductance, li(3). Unlike a previous ITER-similar current ramp-up experiment [2], one equivalent neutral beam source, P_{NBI}=1.8 MW, was injected starting at t=0.3 sec to roughly equilibrate the ion and electron temperatures during the rise time, as well as to allow continuous diagnosis with Charge Exchange Recombination spectroscopy (CER), Motional Stark Effect (MSE), and Beam Emission Spectroscopy (BES) for later transport and simulation analysis. Sawteeth begin shortly after flat-top at t=1.5 sec., as seen on core T_e and T_i measurements. Plasma inductance, calculated from EFIT using MSE ranges from 0.5-0.9 during ramp-up, while q_{95} evolves down towards the ITER steady value of 3.1. Energy confinement improves steadily throughout the ramp-up as both density increases and q_{95} is reduced. Three times of interest have been selected for this study at t=0.4, 0.7 and 1.5 sec as representing early phase, mid-way and flattop transition times at which the plasma current was 0.5, 0.8 and 1.6 MA, respectively, in L-mode plasmas, matching the expected ITER current ramp conditions.

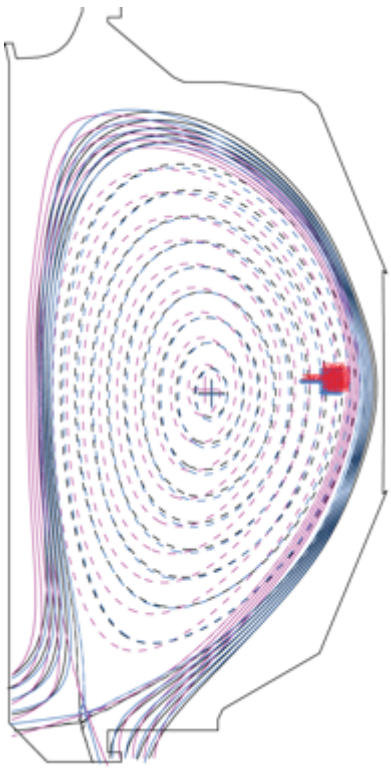

FIG. 2. Magnetic equilibrium calculated using MSE at the three times of interest during ramp-up: t_1=0.4 s (red), t_2=0.7 s (blue), t_3=1.5 s (black). One position of the 2D BES diagnostic array is also shown at the outboard midplane.

The magnetic equilibrium is the standard “ISS” (ITER Similar Shape) used on DIII-D, which is slightly

adjusted to allow for good pumping of the lower outer divertor leg. The discharge starts on the inner wall and establishes the lower divertor starting at 0.24 sec. The shape evolves slightly during the ramp-up at the three times of interest, which are shown in Fig. 2; the outboard midplane position of the separatrix shifts outward several cm during the ramp-up.

The plasma maintains approximately equilibrated electron and ion temperature across the profile during the times of interest during the current ramp, as shown in the profiles in Fig. 3 (a) & (b) at the same three times of interest, showing a monotonic increase in temperatures. The inferred electron and ion thermal diffusivities from ONETWO [13] transport analysis are shown in Fig. 3(c) & (d) and illustrate non-monotonic behaviour with time. Because of potentially small errors in the large electron-ion thermal exchange term, the ion thermal diffusivity appears to go negative towards the edge, whereas electron thermal diffusivity appears to increase significantly. The thermal diffusivities are initially low at the first time (0.4 s), when temperature gradients are lower, but the gradients are increasing rapidly. Calculations shown later suggest that turbulence growth rates are also lower during this phase, potentially consistent with lower turbulent transport. At 0.7 sec, thermal diffusivities for both ions and electrons are at the largest of the three times, as the profiles steepen and multiple energy confinement times have passed. Diffusivities then fall as the plasma achieves current flattop and highest energy confinement during the ramp. The density and safety factor profiles are also shown in Fig. 3 indicating the monotonic q-profiles and uniformly increasing density. The near scrape-off-layer electron temperature profile, obtained from a reciprocating Langmuir probe [14], is shown in Fig. 4, which shows different behavior, with the SOL temperature and width decreasing as current increases, consistent with SOL width scaling with I_P and improved thermal confinement.

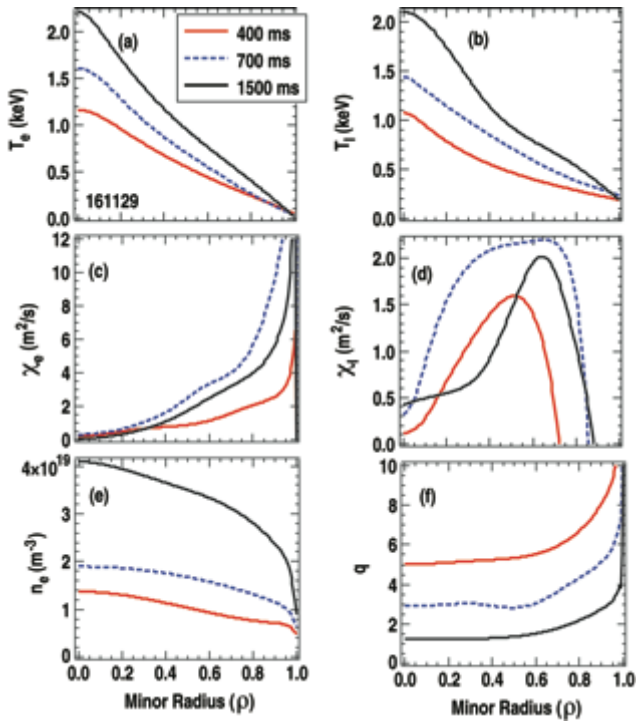

FIG. 3. Profiles of a) electron temperature, b) ion temperature, c) electron thermal diffusivity, d) ion thermal diffusivity, e) density, f) safety factor, q, at three times during current ramp discharge, t_1=400 ms (I_p=0.5 MA), t_2=700 ms (I_p=0.8 MA), and t_3=1500 ms (I_p=1.6 MA).

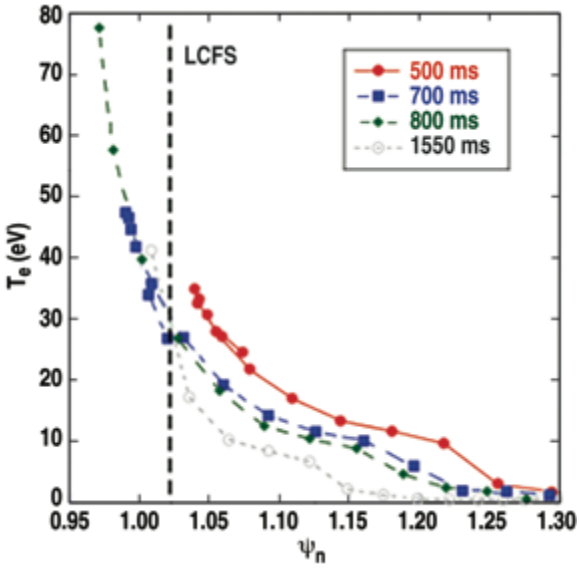

FIG. 4. Profiles of T_e at several times during I_P ramp (reciprocating Langmuir probe).

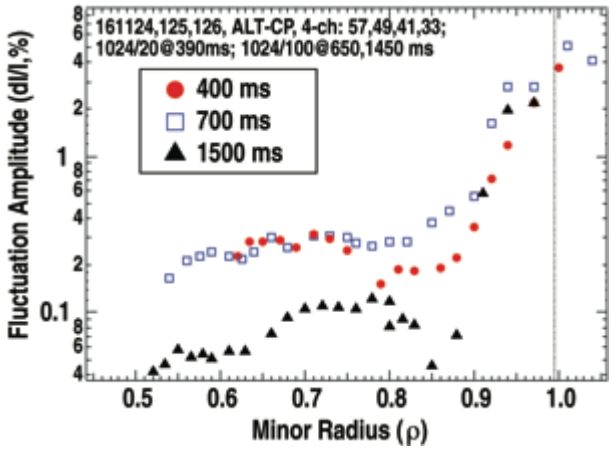

FIG. 5. Fluctuation amplitude profile measured with BES at 400 ms (red circles), 700 ms (blue open squares), and 1500 ms (black triangles) during current ramp; fluctuations were integrated over specific spatially and temporally varying frequency ranges between 5 and 400 kHz.

3. Fluctuation Behavior During Current Ramp

A principal goal of this experiment was to obtain comprehensive fluctuation measurements to compare with models and simulations. A related goal was to identify the source of the transport anomaly described in the Introduction that is observed during ramp up. As will be shown, low-wavenumber density fluctuations exhibit rapidly changing spectral and spatial characteristics and amplitude during the current ramp-up phase of these discharges.

Measurements of the 2D low-wavenumber density fluctuation properties were obtained across the outer half-radius with Beam Emission Spectroscopy [15]. Three nearly identical discharges were performed, and the 2D BES measurement array was spatially moved between shots to cover the range $0.5 < \rho \leq 1$. The fluctuation spectra and amplitude vary over orders of magnitude during the ramp up and across the radius. The fluctuation amplitude profile is shown in Fig. 5, illustrating several unique properties of the dynamically evolving turbulence. For the first measurement at t=0.4 sec, a 20 ms time window is averaged since the plasma evolves quickly at this point; for the later times, t=0.7 and t=1.5 sec., a 100 ms time window is averaged to improve signal-to-noise during these more slowly evolving times; comparison of the turbulence at the beginning and end of these time windows shows little change, justifying this time averaging. The ***ExB*** Doppler shift of the fluctuation spectrum varies with time as toroidal and poloidal rotation and pressure gradient evolve. The spectral range integrated for each measurement is therefore adjusted to the appropriate spectral range for each radius. Inside of ρ=0.9, the normalized fluctuations, ñ/n, are generally below 1%. The fluctuations exhibit a curious minimum between 0.75 and 0.9 but then rise inside and outside of this zone at t=0.4 sec. (measurements were only available into ρ=0.6 due to the smaller plasma at this early time). At t=0.7 sec, fluctuations are flat or monotonically increasing radially and at their largest relative magnitude. Note that this higher fluctuation amplitude correlates with the highest thermal diffusivities in Figs. 3 (c) & (d), suggesting that these fluctuations are responsible for a significant fraction of the

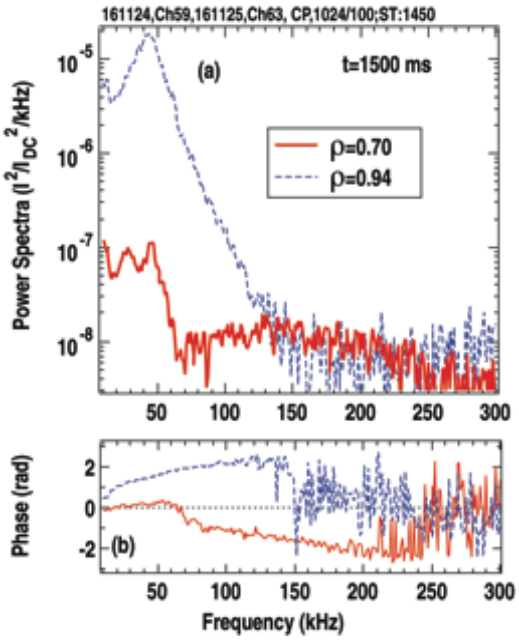

FIG. 6. Comparison of the density fluctuation spectra (logarithmic) from BES at two radii during current flattop, t=1.45-1.55 sec., a) cross power spectra of two poloidally-displaced channels (ΔZ=1.3 cm), and b) the associated cross-phase (positive phase reflects advection in electron diamagnetic direction, negative in ion direction).

turbulent transport.

At the later time of t=1.5 sec, the fluctuation amplitude is reduced to its lowest level, and like at t=0.4 sec, they exhibit a curious local minimum between 0.8<ρ<0.9. Notably, the ion and electron thermal transport are lower than at 0.7 sec., but do not exhibit a minimum at 1500 ms, so there is not an exact quantitative correlation between low-k density fluctuations and ion and electron thermal transport. This may result from changes in the unmeasured temperature, potential and magnetic fluctuations, as well as higher wavenumber turbulence, such as might result from electron modes, that isn't measured but may contribute significantly to transport. Increased collisional coupling between ions and electrons in the cooler edge region could facilitate transport of ion heat by electron modes.

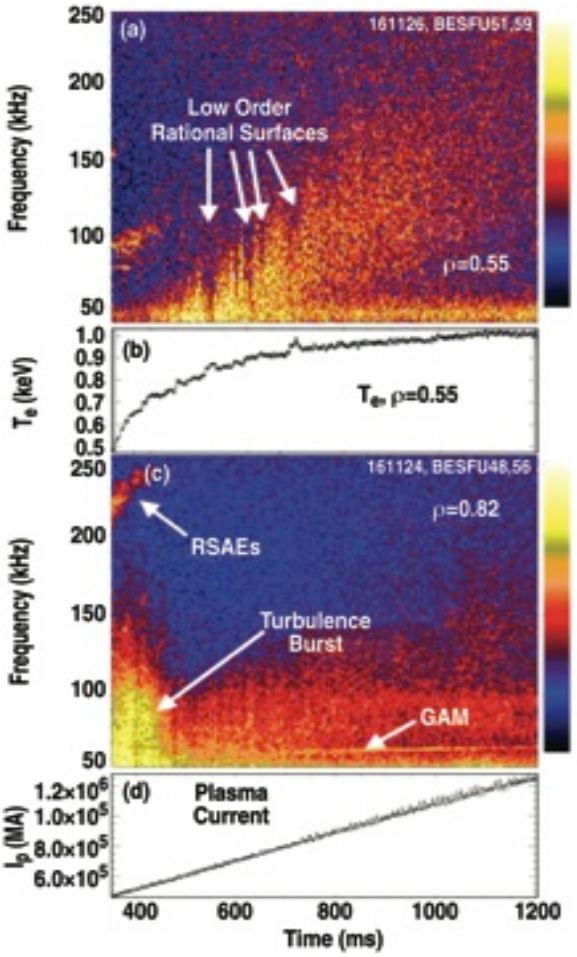

FIG. 7. (a) Spectrogram of BES density fluctuations during I_p-ramp at ρ=0.55-0.65, (b) T_e at ρ=0.55, (c) density fluctuations at ρ=0.79-0.95 , (d) plasma current.

The fluctuations at the outer radii, 0.9<ρ≤1 exhibit distinctly different behavior from the core fluctuations in these L-mode edge plasmas. Besides being much larger in amplitude (ñ/n<10%), fluctuations in this edge zone show much less change with time. Furthermore, these fluctuations are found to propagate in the opposite poloidal direction compared with the core fluctuations, which suggests they may be driven by a different instability; some studies suggest that resistive ballooning modes may dominate the cool edge plasma [16]. This is illustrated in Fig. 6, where fluctuations exhibit a much larger amplitude near the edge than in the core (Fig. 6(a)). The poloidal advection for the core fluctuations is dominated by the ExB velocity, which results primarily from the co-current toroidal velocity from neutral beam injection. The measured poloidal velocity of turbulence typically compares very well to the local ExB velocity [17], which should be the case assuming the intrinsic mode velocity is small (typical). This results in the increasing negative cross-phase with frequency measurement (propagation in the ion diamagnetic direction) for fluctuations at ρ=0.7 (fluctuations below 60 kHz are dominated by beam noise and thus near zero (Fig. 6(b)). For the edge region, outside of ρ=0.9, fluctuations are found to advect in the opposite or electron diamagnetic direction, demonstrated by the positive and increasing phase angle with frequency in Fig. 6(b). This dual-mode behavior is often seen near the edge in plasmas with the ion grad-B drift towards the X-point [18], as is the case here.

Time-resolved spectrograms of density fluctuations reveal several unique turbulence features that are largely consistent with evolving transport behavior. Fig. 7 shows a spectrogram of the density fluctuations at ρ=0.55-0.65 (Fig. 7(a)) and ρ=0.79-0.95 (Fig. 7(c)). At ρ=0.55-0.65,

fluctuations generally decrease in amplitude with time, and fluctuation frequency increases with increasing rotation (Doppler-shift). Each BES spatial is fixed in space and so drifts radially in the plasma frame over the course of the time window shown due to shape and magnetic equilibrium evolution over the range indicated. Of particular note, transient windows of suppressed fluctuations are observed during ramp-up, which correspond to low-order-rational q-surfaces entering the core plasma [19] that are likely associated with regions and times of improved transport; the local electron temperature, in Fig. 7(b), exhibits transient increases during these periods of reduced fluctuations [20]; these times are indicated by white arrows in Fig. 7(a). The large reduction in fluctuations seen in Fig. 5 near $0.8<\rho<0.9$ may correlate with and result from the q=m/n=3/1 surface that is located in this region at this time. The effects of low-order rational q-surfaces are observed over a moderate radial range that extends well beyond the position where the q-surface enters the plasma. At a radius of near $\rho=0.82$ (Fig. 7(c)), significantly different behavior is observed: a very large amplitude burst of low-frequency turbulence (5-80 kHz) occurs early in the ramp, simultaneously with a set of Reversed-Shear Alfven Eigenmodes (RSAEs) at 150-200 kHz. A Geodesic Acoustic Mode (GAM) is also evident near 15 kHz, with frequency increasing with time as T_e and sound speed increase [21].

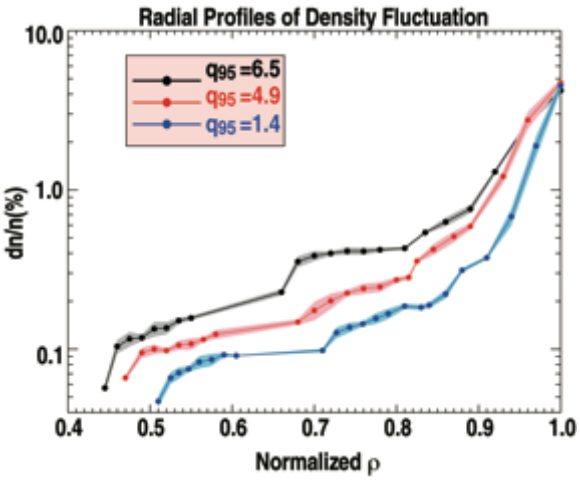

FIG. 8. Comparison of density fluctuation profiles (BES) from three different discharges with different q_{95} during a quasi-steady phase of the plasma (not current ramp). Shots 150137, 150140, 150143

The transient periods of very low turbulence near low-order rational surfaces and at the outer radii shown in Fig. 5 indicates behaviour that is not captured by models used in transport simulations. This reduced turbulence corresponds with lower transport, as illustrated by the transient increases in electron temperature (Fig. 7(b)). If the transient reductions that occur near the multiple low-order rational surfaces that enter and propagate radially outwards were properly captured by the models, the net effect would be to increase the predicted outer electron temperature profile and potentially bring the models into closer agreement with observed transport. This is especially important to modelling the ramp-up given the stronger impact of the electron temperature in the outer half radius to current penetration, q-profile evolution, plasma inductance and ohmic flux consumption.

A related experiment, performed during quasi-steady plasma conditions, not during the current ramp-up, demonstrated that increasing the safety factor increases fluctuation amplitude, as shown in Fig. 8, generally consistent with the strong I_P scaling of energy confinement; measured thermal energy confinement likewise decreases with increasing q_{95}. GAMs and low frequency zonal flows also vary in amplitude with q_{95}. Interestingly, though, these dependencies are somewhat different from the dynamically evolving properties observed during this current ramp experiment. Specifically, the regions of very low fluctuations observed near $0.8<\rho<0.9$ during early and late ramp up times (Fig. 5) are not observed in the quasi steady plasmas, and fluctuations don't exhibit monotonic behavior radially during the changing q of the ramp; they generally increase monotonically with radius during steady plasma conditions. The current ramp-up time scale (~1 sec) is much slower than the turbulence time scales (~10-100 microsec), but comparable to the energy confinement

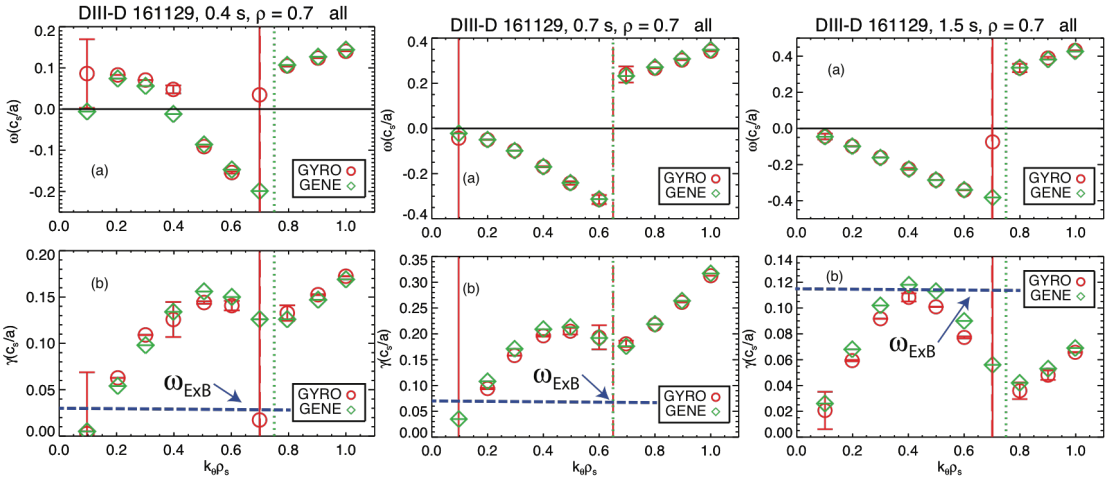

FIG. 9. Calculated linear growth rates at ρ=0.7 from GYRO and GENE at the three times of interest, a) t=0.4 sec, b) t=0.7 sec, c) t=1.5 sec. Red and green vertical lines indicate changing sign of dominant instability frequency and therefore change from ion to electron modes; ExB shearing rates are also indicated as dashed blue lines for each time.

time (50-100 ms) over which profiles evolve significantly, and so differences in fluctuation behavior most likely arise from differing profiles and equilibria between ramp-up and steady-state conditions. These observations suggest that the dynamically evolving parameters lead to distinctly different fluctuation and transport behavior.

4. Transport Modeling of Ramp-up Phase

Linear growth rates have been calculated for these discharges with GYRO [22], CGYRO [23] and GENE [24], and show robustly unstable ITG, TEM, and ETG modes; growth rates vary significantly in time and location during ramp up. The mode frequency and growth rate spectra are shown in Fig. 9, demonstrating that the dominant low-wavenumber instability varies from a TEM (indicated by positive frequencies) to an ITG (negative frequencies) at ρ=0.7 as time evolves during the current ramp-up (only lower-k growth rates shown). Furthermore, the magnitudes of the growth rates show qualitative similarity to fluctuation amplitude and transport behavior. The growth rates achieve a maximum at t=0.7 sec, when low-wavenumber fluctuations reach a maximum normalized value, and growth rates are at a minimum at t=1.5 sec, when measured low-wavenumber fluctuations are also at a minimum at ρ=0.7 and thermal transport is lower than it was at t=0.7 sec. Since a single co-current neutral beam source was injected into these plasmas, net injected torque causes relatively slow to modest co-current toroidal rotation and corresponding ExB shear. The normalized total ExB shearing rates (calculated including toroidal and poloidal rotation and pressure gradient using the carbon ion radial force balance equation) are shown in each of the growth rate graphs in Fig. 9 as a horizontal blue dashed line. At t=400 ms and 700 ms, the shearing rates are quite low relative to the respective growth rates, but at t=1500 ms, the shearing rate is comparable to the growth rates. This may partially explain the significantly lower measured turbulence at ρ=0.7 and reduced heat transport at the later time. Nonlinear simulations are in progress and will be quantitatively compared with measurements of transport and fluctuations in a future publication.

The dependence of linear growth rates on the local safety factor value was computed with CGYRO, and is shown in Fig. 10. CGYRO is a nonlinear initial-value continuum gyrokinetic code, optimized for solving the collisional delta-f gyrokinetic-Maxwell equations [23]. It is a successor to the GYRO code, but uses the velocity-space coordinate system of the

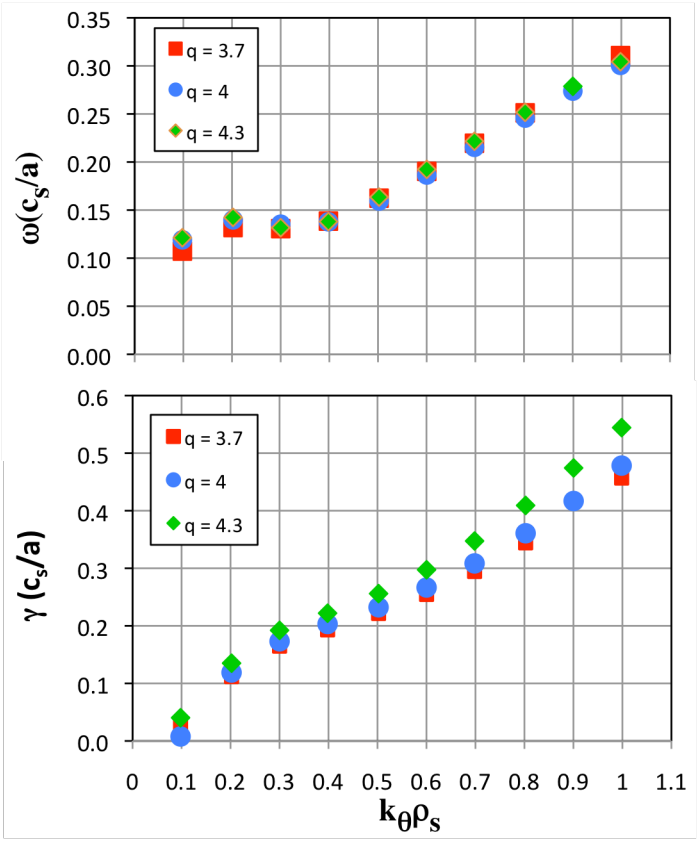

FIG. 10. Comparison of mode frequency and growth rate spectra with CGYRO for three values of local safety factor, q, at ρ=0.75, t=0.7 sec.

neoclassical code, NEO, which allows for more accurate descriptions of collisional dynamics. The reference plasma conditions were those at ρ=0.75 at t=0.7 sec. to discern whether any significant changes are observed near low-order rational surfaces, q=4 in this case. The frequencies show very little dependence on q, with other local plasma parameters being held constant. The growth rates show a very weak dependence, increasing slightly with q, which is qualitatively consistent with the increased fluctuations and transport at higher q (Fig. 8). This weak and monotonic dependence demonstrate that calculated local linear growth rates are not affected by the low-order rational (q=4 here), relative to nearby values of q. It's possible then that the observed reductions of turbulence near low-order rational surfaces results from global and/or nonlinear effects; related profile corrugations were observed in previous GYRO simulations near low-order rational surfaces [25] as a result of a time-averaged zonal flows that form near q=2 and may be associated with the formation of an internal transport barrier.

5. Summary

Turbulence has been shown to vary significantly in space and time during the current ramp-up phase of ITER-like plasmas on DIII-D. This behaviour exhibits several unique characteristics that suggest a complex behaviour that may cause the transport anomalies observed in previous discharge modelling, including the discrepancy between measured and predicted electron temperature profiles in the outer half radius. There appears to be a strong interaction between the evolving electron temperature and thermal transport, safety factor (q), and low-order rational surfaces. Of particular note, very low levels of broadband turbulence are observed at outer radii during early and late times of the current ramp. This could lead to reduced transport and increased electron temperatures, which might explain the discrepancies between CORSICA modelling and the higher T_e measurements in the outer radii. Furthermore, numerous low-order rational q-surfaces enter the plasma during the ramp-up, which correlate with transient suppression of turbulence and transport. Future quantitative simulations of these fluctuation measurements may explain discrepancies between existing transport models and T_e measurements during the ramp-up phase and thereby lead to improved predictive models.

6. Acknowledgements

This work supported by the US Department of Energy under DE-FG02-89ER53296[1], DE-FG02-08ER54999[1], DE-FG03-97ER54415[2], DE-FG02-07ER54917[3], DE-FG02-06ER54871[3], DE-FG02-08ER54978[4], DE-FC02-04ER54698[5] and DE-FG02-08ERA54984[6]. Data shown in this paper can be obtained in digital format by following the links at https://fusion.gat.com/global/D3D_DMP.

References

[1] Shimada M. et al Nucl. Fusion **47,** S1 (2007).

[2] G.L. Jackson, T.A. Casper, T.C. Luce *et al.*, Nucl. Fusion **48**, 125002 (2008).

[3] G.L. Jackson, T.A. Casper, T.C. Luce *et al.*, Nucl. Fusion **49**, 115027 (2009).

[4] I. Voitsekhovitch, A. C. C. Sips, B. Alper, M. Beurskens *et al.*, Plasma Phys. Control. Fusion **52**, 105011 (2010).

[5] F. Imbeaux, J. Citrin, J. Hobirk *et al.*, Nucl. Fusion **51**, 083026 (2011).

[6] T.C. Luce, D.A. Humphreys, G.L. Jackson, W. Solomon, Nucl. Fusion **54**, 093005 (2014).

[7] T.A. Casper, W.H. Meyer, G.L. Jackson *et al.*, Nucl. Fusion **51** , 013001 (2011).

[8] D.R. Mikkelsen, R.V. Budny, T.A. Casper, ITPA Transport Final Report TC-20 (2013).

[9] C. Holland, A. White, G.R. McKee, Phys. Plasmas **16**, 052301 (2009).

[10] J. E. Kinsey, G. M. Staebler, J. Candy, C. C. Petty, T. L. Rhodes, and R. E. Waltz, Phys. Plasmas **22**, 012507 (2015).

[11] T. Görler, A. E. White, D. Told, F. Jenko, C. Holland, T.L. Rhodes, Phys. Plasmas **21**, 122307 (2014).

[12] N.T. Howard, A.E. White, M. Greenwald, M.L. Reinke, J. Walk, C. Holland, J. Candy, T. Görler, Phys. Plasmas **20**, 032510 (2013).

[13] St. John, H, Taylor, T S, Lin-Liu, Y R, Turnbull, A.D., Plasma Physics and Controlled Nuclear Fusion Research **3**, 603 (1994).

[14] Watkins, J. G., Salmonson, J., Moyer, R., Doerner, R., Lehmer, R., Schmitz, L., & Hill, D. N., Rev. Sci. Instrum. **63**, 4728 (1992).

[15] G.R. McKee, R.J. Fonck, M.W. Shafer I.U. Uzun-Kaymak, Z. Yan, Rev. Sci. Instrum. **81**, 10D741 (2010).

[16] C. Bourdelle, X. Garbet, R. Singh, L. Schmitz, Plasma Phys. Control. Fusion **54**, 115003 (2012).

[17] M.W. Shafer, R.J. Fonck, G.R. McKee *et al.*, Phys. Plasmas **19**, 032504 (2012).

[18] C. Fenzi, G.R. McKee, R.J. Fonck *et al.*, Phys. Plasmas **12**, 062307 (2005).

[19] M.W. Shafer, G.R. McKee, M.E. Austin *et al.*, Phys. Rev. Lett. **103**, 075004 (2009).

[20] M.E. Austin, K.H. Burrell, R. Waltz *et al.*, Phys. Plasmas **13**, 082502 (2006).

[21] G.R. McKee, R.J. Fonck, M. Jakubowski *et al.*, Phys. Plasmas **10**, 1712 (2003).

[22] J. Candy, R.E. Waltz, J. Comp. Phys. **186**, 545 (2003).

[23] J. Candy, E.A. Belli, R.V. Bravenec, J. Comp. Phys. **324**, 73 (2016).

[24] T. Görler, X. Lapillonee, S. Brunner, T. Dannert, F. Jenko, F. Merz, D. Told, J. Comp. Phys. **230**, 7053 (2011).

[25] R.E. Waltz, M.E. Austin, K.H. Burrell, J. Candy, Phys. Plasmas **13**, 052301 (2006).